https://doi.org/10.5194/egusphere-2026-3871
Preprint. Discussion started: 8 July 2026

Title:

Impact of mean sea level rise on storm surges and tide-surge interaction in the German Bight

Authors: Xin Liu, Lidia Gaslikova, and Ralf Weisse

Institute of Coastal Systems - Analysis and Modeling, Helmholtz-Zentrum Hereon, Max-Planck-Str. 1, 21502 Geesthacht, Germany

Correspondence to: Xin Liu (xin.liu@hereon.de)

Abstract. Changes in mean sea level not only directly contribute to extreme water levels (EWLs) but also modulate tidal dynamics, storm surges, and their nonlinear interactions, particularly in shallow shelf seas. This study investigates how sea level rise (SLR) affects storm surges and tide-surge interaction (TSI) in the German Bight, with the aim of assessing the validity of linear approaches commonly used to estimate EWLs in coastal risk studies. A hydrodynamic model was used with a set of controlled experiments for the period 1981–2010, explicitly separating tidal and atmospheric contributions and their interactions, additionally comparing present-day conditions with a +1 m SLR scenario. We demonstrate the importance of tidal phase in modulating the magnitude and timing of storm surges via TSI. The strength of this interaction increases with storm surge height, while its dependence on high tide magnitude and tidal range is comparatively weak. Under SLR, TSI weakens mainly because increased water depth reduces bottom friction, diminishing its dampening effect by about 25 %. Moreover, storm surge heights show a slight decrease, primarily due to phase shifts caused by faster wave propagation in deeper water and reduced wind stress efficiency acting upon a thicker water column. Overall, the nonlinear effects of SLR on storm surges and TSI are small, on the order of a few centimeters for 1 m SLR, relative to the direct contribution of SLR. This supports the use of linear superposition for many practical applications, while highlighting that nonlinear interactions introduce systematic, process-based adjustments relevant for precise EWL estimates.

https://doi.org/10.5194/egusphere-2026-3871
Preprint. Discussion started: 8 July 2026

1 Introduction

Extreme water level (EWL) is a combination of many factors, including contributions from storm surges, tides, wave setup, mean sea level (MSL) changes and interactions among those factors. In the North Sea, on short-time scales, storm surges occurring on top of high tides are the primary cause of EWL events. On long-time scales, the observed increase in EWL is mostly associated with the long-term increase in MSL (Haigh et al., 2010; Weisse et al., 2012; Weisse et al., 2014). By 2100, EWL in the North Sea is projected to increase by nearly 1 m under RCP8.5, mainly due to the corresponding rise in MSL (Vousdoukas et al., 2017).

According to the IPCC Sixth Assessment Report (AR6), future sea level rise (SLR) in the North Sea will be similar to the global mean projections, with slightly higher rates along the southern North Sea coasts (Fox-Kemper et al., 2021; Garner et al., 2021; Kopp et al., 2023). SLR raises the baseline water level, so even moderate storm surges can trigger extreme impacts and increase the frequency of extremes (Lowe et al., 2001; Hunter, 2010; Taherkhani et al., 2020). Flood risk assessments often account for this by linearly adding SLR to present-day EWL estimates. At the same time, rising water depth alters tides, storm surges and their interactions, especially in shallow regions (Idier et al., 2019). These nonlinear effects remain insufficiently understood and are examined in this study.

The shallow coastal areas of the North Sea are known for large tide-surge interactions as well as tide and MSL interactions (e.g. Bruss et al., 2011; Pickering et al., 2012; Idier et al., 2017). Because MSL is rising rapidly and often omitted from EWL projections, it is crucial to determine whether SLR scales linearly with EWL or whether interactions substantially alter this simple relationship. Nonlinear interactions among these components may either amplify or reduce total water levels, depending on the region, tidal phase or storm type (Horsburgh and Wilson, 2007; Bruss et al., 2011; Arns et al., 2017; Zhang et al., 2017; Arns et al., 2020). These interactions are essential for understanding water level dynamics and for producing reliable EWL estimates for design and operational forecasting (Zijl et al., 2013; Arns et al., 2017; Arns et al., 2020).

Several studies have therefore examined how such nonlinear processes manifest along the North Sea coast. An ensemble study from *Sterl et al.* (2009) showed that no significant change in EWLs on top of SLR along the Dutch coasts. Yet for the shallow areas of the North Frisian Wadden Sea, increases in EWLs beyond SLR were found and attributed mainly to the increase in high tide (Arns et al., 2015).

Furthermore, it is useful to estimate how individual components of water level respond to SLR. Many previous studies have investigated tide changes in response to SLR, which have been recognized as spatially incoherent on a global scale (see Idier et al., 2019 and references therein). Even for regional scale, e.g., the North Sea, the results differ substantially (Pickering et al., 2012; Ward et al., 2012; Pelling et al., 2013; Idier et al., 2017). In particular, for the German

https://doi.org/10.5194/egusphere-2026-3871
Preprint. Discussion started: 8 July 2026

Bight, studies have reported an increase in the semidiurnal M2 amplitude (Pickering et al., 2012) and high tide levels (Idier et al., 2017), whereas *Ward et al.* (2012) found a decrease in M2 amplitude in response to 2 m SLR. *Pelling et al.* (2013) attributed these differences to the model formulation, specifically whether flooding of low-lying coastal areas is allowed in the model. The newly flooded cells create new shallow areas of high dissipation that counteracts the general decrease of dissipation due to SLR. *Rasquin et al.* (2020) further attributed the substantial discrepancies in the results to the importance of the bathymetry resolution, especially in flat intertidal areas, for modelling the tidal response to SLR.

While tidal changes under SLR have received considerable attention, the indirect effect of SLR on storm surges (driven purely by meteorological forcings) remain less well understood. There are studies that use non-tidal residual (e.g. Lowe et al., 2001; Arns et al., 2015) or skew surge (e.g. Sterl et al., 2009) to assess surge changes in response to SLR. Minor changes are found for the shelf region around the United Kingdom and along the Dutch coast (Lowe et al., 2001; Sterl et al., 2009), while a reduction in surge height was reported for the shallow areas of the North Frisian Wadden Sea. There, deeper water reduces the effectiveness of wind stress in dragging water columns and thus leads to the decrease in surge height, despite reduced bottom friction and lower energy dissipation (Arns et al., 2015).

Because tides and surges do not evolve independently, their interaction represents a further key process influencing EWLs. Earlier studies suggest that the tide-surge interaction (TSI) is not negligible for reliable EWL predictions (Horsburgh and Wilson, 2007; Olbert et al., 2013; Arns et al., 2020). Its magnitude varies across continental shelves (Arns et al., 2020) and within the North Sea, including the UK coast (Prandle and Wolf, 1978; Horsburgh and Wilson, 2007) and the English Channel (Haigh et al., 2010; Idier et al., 2012). In the North Sea, storm surges typically peak on a rising tide with reduced surge heights due to nonlinear TSI (Prandle and Wolf, 1978). *Horsburgh and Wilson* (2007) attribute this to tidal phase shift caused by faster wave propagation in deeper water and tidally modulated surge generation, with stronger surges at low water because wind stress is more effective in shallow depths. Additionally, local variations in TSI appear across tide gauges, possibly related to different tidal ranges and shape of the coastline. No significant long-term SLR related changes in TSI have been detected in recent decades (Haigh et al., 2010; Feng et al., 2019). This study therefore focuses on TSI in the German Bight and, in particular, its response to future SLR.

Given the importance of these nonlinear mechanisms and the remaining uncertainties, our study quantifies the indirect impact of SLR on EWLs in the German Bight, with a particular focus on storm surges and TSI. Rather than providing full projections of EWLs, we concentrate on how SLR modifies these components, in order to assess the validity of commonly applied linear superposition approaches. While TSI describes the nonlinear superposition of tides and meteorologically driven surges under present-day conditions, we additionally investigate how this interaction itself changes when water depth increases due to SLR. To disentangle these

https://doi.org/10.5194/egusphere-2026-3871
Preprint. Discussion started: 8 July 2026

processes, we conduct a suite of targeted sensitivity experiments with a hydrodynamic model and complement them with statistical analyses. Section 2 outlines the model setup and experimental design. Section 3 presents TSI and the resulting changes in TSI and storm surges under SLR, followed by a discussion in Section 4. Section 5 summarizes the key findings.

2 Model, Definitions and Experiments

2.1 Model

The experiments used the barotropic hydrodynamic model TRIM-NP (Tidal Residual and Intertidal Mudflat Nested and Parallelized) (Casulli and Stelling 1998; Kapitza, 2008; Pätsch et al., 2017) on a Cartesian Arakawa-C grid allowing flooding and drying of grid points. The bottom friction is parameterized following a depth-dependent Manning-Chezy formulation, and air-sea interaction is represented by bulk parametrizations for the wind components and sea level pressure. The drag coefficient of wind stress is formulated according to *Smith and Banke* (1975). The model domain covers the North Sea and adjacent parts of the northeast Atlantic with 12.8 km spatial resolution, with a nested grid refinement down to 1.6 km in the German Bight. Tidal forcing is applied at the open boundaries using FES-2004 global tidal reanalysis (Lyard et al., 2006), and atmospheric forcing comes from hourly coastDat-2 COSMO-CLM 10-meter wind components and sea level pressure fields (Geyer, 2014). All experiments described below were run for 1981–2010, and model output was stored hourly.

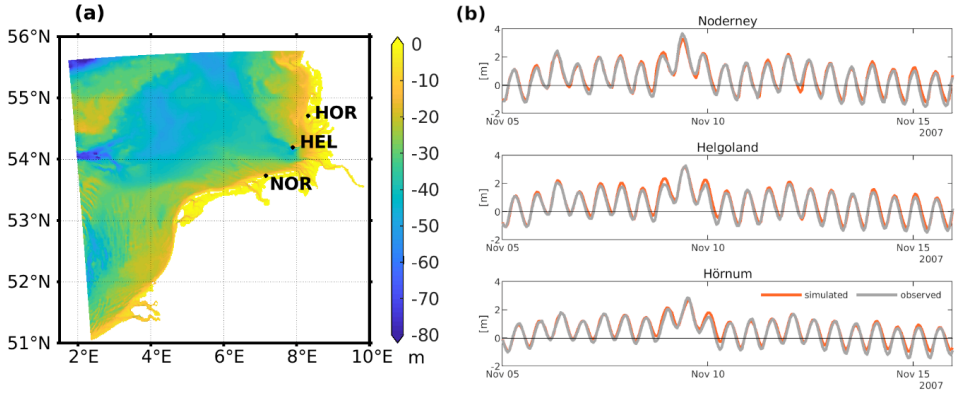

Figure 1. (a) Model domain and the three selected locations (Helgoland, Norderney and Hörnum) in the German Bight. (b) Modelled (gray) and observed (red) water levels for the event on 9 Nov. 2007 at three stations.

The model has been previously validated against observations and applied in a wide range of studies (e.g. Weisse et al., 2015; Meyer and Gaslikova, 2024). For the present configuration, model performance was evaluated over the final ten years of the simulation period (2001–

https://doi.org/10.5194/egusphere-2026-3871
Preprint. Discussion started: 8 July 2026

2010). The validation was conducted by comparing simulated water levels with tide gauge observations at three locations along the German coast: Norderney, Helgoland, and Hörnum (Fig. 1a). These stations are representative for storm conditions in the southern, central, and northern German Bight, respectively, and are used in the subsequent analysis presented in this paper.

The comparison was performed for hourly water levels, high water levels, and hourly non-tidal residuals (NTRs). The NTRs were derived by subtracting the tidal signal, estimated using the U-Tide harmonic analysis Matlab package (Codiga, 2011), from the corresponding observed or modelled total water levels. Model skill was quantified using the Pearson correlation coefficient (r), the absolute root mean square error (RMSE), and the RMSE expressed as a percentage of the maximum observed water level (or NTR) (Table 1), while Fig. 1b provides a visual comparison of modeled and observed water levels.

The model shows good agreement with observations at all three tide gauges for all considered water level components. For hourly water levels, Pearson correlation coefficients are high, ranging from 0.97 at Hörnum to 0.98 at Helgoland, with RMSE values between 0.2 m and 0.23 m, corresponding to 6 % of the maximum observed water level. High water levels are also well reproduced, with correlation coefficients close to 0.9 at all stations and comparatively low RMSE values (0.16 m), amounting to 4–5 % of the highest observed levels. Performance for the hourly NTRs is also robust, with correlations between 0.86 and 0.89 and RMSE values of about 0.16 m (5–6 % of the maximum observed NTR). Overall, the validation results indicate a consistently high model skill across the German Bight, with only moderate spatial variations between the southern (Norderney), central (Helgoland), and northern (Hörnum) stations. The discrepancies can be partly attributed to uncertainties in the atmospheric forcing, as discussed in *Meyer and Gaslikova* (2024), and in part to the relatively coarse horizontal resolution of the model (1.6 km), limiting the performance especially in the wide shallow areas and intertidal flats. The present model configuration therefore represents a deliberate trade-off between accuracy and computational efficiency, which is necessary to enable the execution of multiple multi-decadal simulations.

Table 1: Comparison with tide gauge observations for 2001–2010.

	water level			**high water**			**non-tidal residuals**		
	r	**RMSE (m)**	**RMSE (%)**	***r***	**RMSE (m)**	**RMSE (%)**	***r***	**RMSE (m)**	**RMSE (%)**
Helgoland	0.98	0.21	6.4	0.90	0.16	4.9	0.88	0.16	6.2
Norderney	0.97	0.23	6.1	0.90	0.16	4.3	0.86	0.16	5.3
Hörnum	0.97	0.20	6.1	0.90	0.15	4.6	0.89	0.16	5.5

https://doi.org/10.5194/egusphere-2026-3871
Preprint. Discussion started: 8 July 2026

2.2 Key terms and definitions

To ensure clarity in interpreting the results, key terms used throughout the text are defined below.

Water level (WL) denotes the observed or total water level, accounting for all contributing components and their interactions**.**

Tide (TIDE) refers to the regular rise and fall of water level caused primarily by the gravitational pull of the Moon and the Sun.

Storm surge (SURGE) is the direct response of water level to strong winds and low atmospheric pressure associated with storms.

Tide-surge interaction (TSI) describes the nonlinear interplay between tides and storm surges. It can raise or lower the total water level relative to their linear superposition, especially in shallow coastal areas.

Non-tidal residual (NTR) represents the combined effects of all non-tidal processes. It is often approximated as the difference between the observed water level and the predicted tide, representing the combined effect of storm surge and TSI (Idier et al., 2019).

Effects of SLR: SLR modifies tidal and surge dynamics through depth-dependent processes. Three SLR-related effects are considered:

- **Impact of SLR on storm surge (ISS)**
- **Impact of SLR on tides (IST)**
- **Impact of SLR on tide-surge interaction (ISTSI)**

They quantify how SLR alters surge height, tide and their nonlinear interactions, respectively.

2.3 Experimental set-up

To separate the contributions of tide, storm surge and their interactions, the model was run in three configurations: **FULL** runs with tidal and atmospheric forcing, **TIDE** runs with tidal forcing only, and **SURGE** runs with atmospheric forcing only. To investigate the potential impact of future SLR, each configuration was simulated under two sea-level conditions: **0 m SLR (…_0)** and **+1 m SLR (…_1)**. SLR of 1 m was chosen to represent a plausible high-end scenario consistent with IPCC AR6 global projections of 0.77 (0.63–1.01) m under SSP5-8.5 by 2100 and regional estimates of 0.85 (0.61–1.61) m for Cuxhaven (Fox-Kemper et al., 2021; Garner et al., 2021; Kopp et al., 2023), as well as other high-end assessments exceeding 1 m (Katsman et al. 2011). In total, six experiments were conducted: **FULL_0, FULL_1, TIDE_0, TIDE_1, SURGE_0**, and **SURGE_1** (Table 2). For example, SURGE_1 represents the surge-only run under +1 m SLR and provides the wind-driven surge together with its interaction with the elevated MSL.

https://doi.org/10.5194/egusphere-2026-3871
Preprint. Discussion started: 8 July 2026

Table 2: Sensitivity Experiments.

EXPERIMENT ID	FORCING INCLUDED	SLR CONDITION	PURPOSE / OUTPUT
FULL_0	Tide + Atmosphere	0 m	Baseline total water level (WL)
FULL_1	Tide + Atmosphere	+1 m	WL under SLR (WL_SLR)
TIDE_0	Tide only	0 m	Baseline tidal signal (TIDE)
TIDE_1	Tide only	+1 m	Tide under SLR (TIDE_SLR)
SURGE_0	Atmosphere only	0 m	Baseline storm surge (SURGE)
SURGE_1	Atmosphere only	+1 m	Storm surge under SLR (SURGE_SLR)

2.4 Computation of residual effects and interaction terms

The following diagnostic quantities were derived from the model simulations defined above.

Tide-surge interaction (TSI)

$$TSI = WL - TIDE - SURGE \quad (1)$$

Positive *TSI* values indicate constructive interaction (amplification), while negative values indicate destructive interaction (reduction).

Non-tidal residual (NTR)

$$NTR = WL - TIDE = SURGE + TSI \quad (2)$$

It should be noted that NTR is not equivalent to storm surge in the presence of TSI, as it also includes the nonlinear interaction term.

Impact of SLR on storm surge (ISS)

$$ISS = SURGE\_SLR - SURGE - SLR \quad (3)$$

This definition isolates the dynamical response of storm surges to SLR, independent of the direct increase in MSL. Negative values indicate that surge height decreases under SLR, such that the water level increase is less than the SLR itself. Positive values indicate that surge height increases, leading to water level changes exceeding SLR alone.

Impact of SLR on tides (IST)

$$IST = TIDE\_SLR - TIDE - SLR \quad (4)$$

Analogously, this definition quantifies the dynamical response of the tidal signal to SLR, excluding the direct effect of the imposed sea-level change.

https://doi.org/10.5194/egusphere-2026-3871
Preprint. Discussion started: 8 July 2026

Impact of SLR on tide-surge interaction (ISTSI)

$$ISTSI = WL\_SLR - WL - SLR - IST - ISS \quad (5)$$

Positive values indicate higher TSI values under SLR, while negative values indicate a decrease in TSI values.

3 Results

Storm surge events were identified using the SURGE_0 experiment, which serves as the baseline for the analysis. This choice ensures that event selection is independent of tidal phase and allows a consistent analysis of phase-dependent interaction effects. The 98th percentile of surge peaks was used as a threshold, and events were declustered to ensure at least 24 hours of separation. The number of detected events varies across locations, with 240, 224, and 213 events detected at three different locations along the German coast: Norderney, Helgoland, and Hörnum, respectively (Fig. 1a). For consistency, the 200 largest events were analyzed at each site, unless otherwise specified. As the results were similar across locations, only the analysis for Helgoland is presented in the paper.

3.1 Tide-surge interaction (TSI)

To assess whether TSI occurs in the region, we first compared the distributions of surge peaks with and without interaction. Figure 2a shows the timing of surge peaks relative to high tides, using surge peaks from the surge-only run (SURGE_0) and the nearest high tides from the tide-only run (TIDE_0). In this configuration, the two runs are independent, so surge peaks should be uniformly distributed over the tide cycle. This is indeed observed: the peaks are almost evenly spread over all hourly bins, and the chi-square test statistic remains well below the critical value, confirming no deviation from a uniform distribution. The test statistic χ^2 is computed as (e.g. Haigh et al., 2010):

$$\chi^2 = \sum_{i=1}^{n}[(N_i - e)^2/e], \quad (6)$$

where N_i represents the number of observed events per time bin i, e is the number of expected events per bin under the null hypothesis of a uniform distribution, and n represents the number of bins (here 13 hourly bands were used). Deviation from a uniform distribution is considered significant at the 95 % level if the test statistic exceeds the critical chi-square value ($\chi^2_{12,0.95}$ = 21), where 12 is number of degrees of freedom.

https://doi.org/10.5194/egusphere-2026-3871
Preprint. Discussion started: 8 July 2026

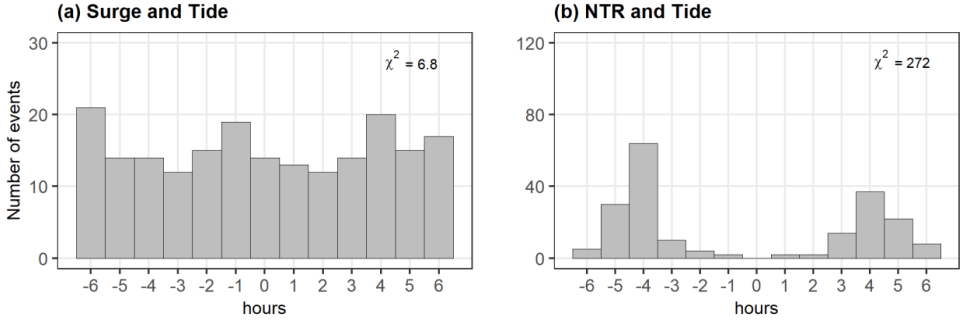

Figure 2. Frequency distribution of (a) surge peaks and (b) non-tidal residual (NTR) peaks relative to the timing of high tide. The corresponding chi-square statistics are shown in each panel.

When NTR peaks were used instead of surge peaks, the distribution is markedly different (Fig. 2b). The NTR peaks occur most frequently on the rising tide, about 4–5 hours before high tides. This is in agreement with previous studies in this region (Horsburgh and Wilson, 2007; Sterl et al., 2009; Idier et al., 2012) and in other shallow regions of the world (Zhang et al., 2017; Koh et al., 2024), which likewise found residual peaks tending to avoid high tides. *Horsburgh and Wilson* (2007) attributed this to phase shift of the tidal signal caused by surge-induced depth changes and to the modulation of surge production by water depth. The contrast between Figs. 2a and 2b demonstrates that NTR is not simply the water level response to atmospheric forcing and that TSI plays a crucial role in shifting the timing of surge peaks. This further confirms that NTR cannot be interpreted as a direct measure of storm surge, as it also contains the contribution from TSI.

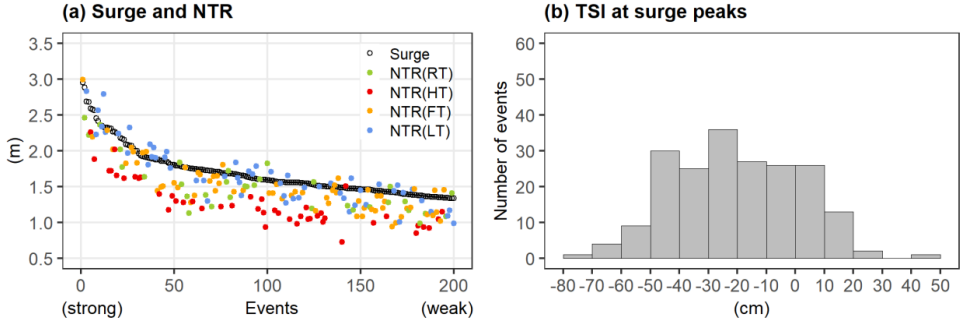

Figure 3. (a) Comparison of surge (black open cycles) and NTR (colored points) at surge peaks, ordered from highest to lowest surge. The NTR values are grouped by tidal phase: rising tide (RT, green), high tide (HT, red), falling tide (FT, orange), and low tide (LT, blue). (b) Frequency distribution of TSI at surge peaks.

https://doi.org/10.5194/egusphere-2026-3871
Preprint. Discussion started: 8 July 2026

Figure 3a shows that surge height and NTR height are only weakly linked. While NTR values generally decrease with decreasing surge height, the NTR values across tidal phases show substantial scatter. NTR at high tide (red) tends to lie near the lower end of the range, while NTR at low (blue), rising (green), and falling tide (orange) more often show higher values. The comparison of surge height and NTR at surge peaks further shows that NTR is generally lower than the corresponding surge height (Fig. 3a), indicating a reduction of water level by TSI at surge peaks. On average, NTR is about 12 % lower than the corresponding surge maxima. This is consistent with the distribution of TSI at surge peaks (Fig. 3b), which is predominantly negative, with values mostly between −54 cm and 14 cm (5^{th}–95^{th} percentiles) and a mean of about −21 cm.

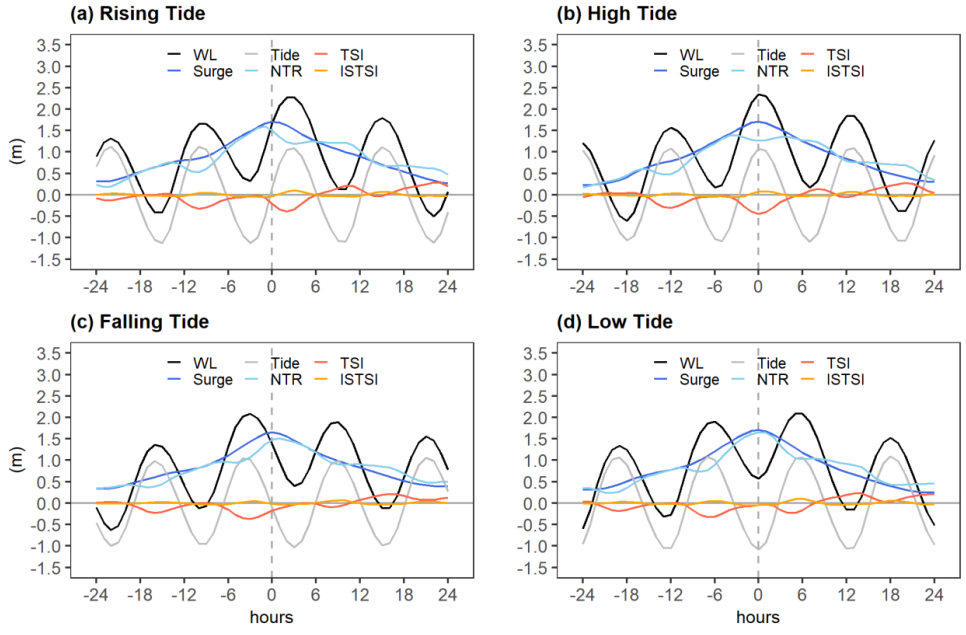

Figure 4. Event-averaged curves for water level (black), tide (gray), surge (blue), NTR (light blue), tide-surge interaction (TSI, red), and the SLR impact on TSI (ISTSI, orange), shown around the surge peak (gray dashed line) for surge peaks occurring during (a) rising tide, (b) high tide, (c) falling tide and (d) low tide.

To examine the phase dependence more systematically, events were grouped by the tidal phase at which the surge peak occurred, and event-averaged curves were constructed (Fig. 4). This is possible because the events are identified with the surge-only run and are therefore not influenced by tidal phase. High and low tides are defined as the tidal maximum and minimum,

https://doi.org/10.5194/egusphere-2026-3871
Preprint. Discussion started: 8 July 2026

including a ±1 hour interval around each. At Helgoland, for example, 33 events occurred at rising tide, 48 at high tide, 62 at falling tide, and 57 at low tide. Across all groups, tide and TSI are generally negatively correlated (gray and red curves), consistent with the behavior described in *Song et al.* (2020) for Bohai Bay in northeastern China. The strongest negative TSI occurs mostly near high tide or on rising tide rather than at surge peak. This is in line with previous studies, showing that the maximum TSI effect does not necessarily coincide with the maximum surge (Rego and Li, 2010; Zhang et al., 2017; Huang et al., 2025).

The negative TSI indicates a dampening effect on surge heights, which is also evident from the comparison between surge and NTR (blue and light blue curves). The NTR values are generally lower than the surge peaks, with the magnitude of the reduction depending on tidal phase. TSI is typically negative during rising surges, reflecting a consistent reduction of surge height, but it can become positive during falling surges, when the interaction can briefly enhance water levels.

The strongest reduction occurs when surge peak coincides with high tide, causing NTR to reach its maximum before or after surge peaks (Fig. 4b). This phase also shows the largest timing shifts, with two clusters around ±3 hours (red points in Fig. 5). When surge peaks occur at low tide (Fig. 4d), the interaction is weak, and NTR peaks lie within about one hour of surge peaks (blue points in Fig. 5). The rising- and falling-tide cases show intermediate reductions (Figs. 4a and 4c), with typical timing shifts of about −1 hour during rising tide and +1 hour during falling tide (green and orange points in Fig. 5). Similar phase-dependent nonlinear effects were reported for Hurricane Rita landfall timing experiments, where low-tide landfalls enhanced and high-tide landfalls reduced total water levels (Rego and Li, 2010).

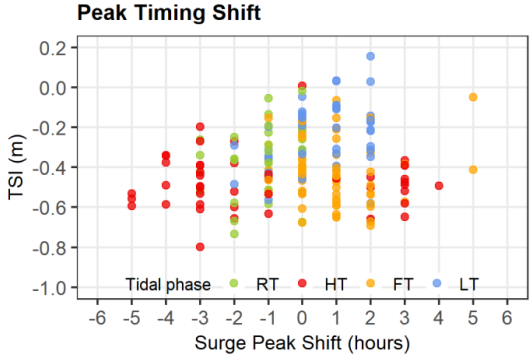

Figure 5. TSI at high tide versus shift in peak timing between NTR and surge ($PT_{NTR} - PT_{Surge}$), conditioned upon tidal phase: rising tide (RT, green), high tide (HT, red), falling tide (FT, orange) and low tide (LT, blue).

https://doi.org/10.5194/egusphere-2026-3871
Preprint. Discussion started: 8 July 2026

The curves in Fig. 4 represent averages across subsets of events. However, the events in each subset show considerable variability in terms of surge and NTR relations. For events occurring near low tide (Fig. 4d), the averaged surge and NTR are close to each other at surge peak, yet more than 40 % of the low-tide cases exhibit positive TSI, meaning NTR exceeds surge (blue points above black cycles in Fig. 3a). From the perspective of the positive TSI events, over half of the events occur when surge peak is near low tide, with the remainder split roughly evenly between rising and falling tides. In contrast, for cases near high tide (red points in Fig. 3a), NTR is consistently lower than surge, confirming that TSI reaches its strongest negative values around high tide and exerts a clear dampening effect on surge maxima. Overall, the results demonstrate that the magnitude and timing of TSI effects are strongly dependent on tidal phase.

We next examine how surge height and tidal range influence TSI. When TSI values are considered at all high tides, regardless of the presence of surge, the distribution is roughly symmetric around zero (not shown). The negatively biased distribution of TSI seen in Fig. 3b appears only under surge conditions. As also shown above, TSI is strongly dependent on tidal phase. To condense the results in the following analysis, the same 200 events (Section 3) are therefore evaluated at the moment of high tide rather than at surge peaks. This approach captures the strongest negative TSI and provides a more relevant basis for EWL estimates, whose peaks typically occur near high tide. As shown in Fig. 6a, TSI becomes more negative as surge height increases, indicating that the dampening effect of TSI tends to strengthen during stronger surges. This is consistent with the expectation that stronger surges generate stronger currents and thus stronger nonlinear interactions, as also noted by *Zhang et al.* (2017).

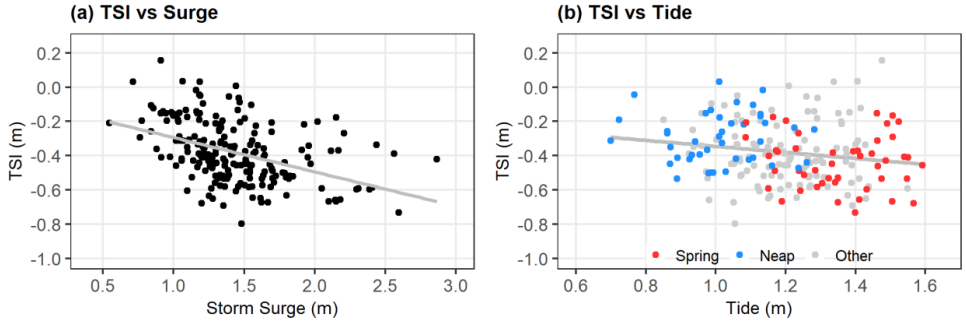

Figure 6. (a) Scatter plot of TSI versus surge height at high tide with fitted regression line. (b) Same as (a), but for the high tide magnitude. Points occurring during spring and neap tides are highlighted in red and blue, respectively.

The magnitude of high tide, defined here as the instantaneous water level at high water in the tide-only run (TIDE_0), and tidal range in general also influence TSI, though less clearly. Compared to the trend for surge height, the dependency of TSI on high tide magnitude is

https://doi.org/10.5194/egusphere-2026-3871
Preprint. Discussion started: 8 July 2026

weaker and more scattered (Fig. 6b). High tide magnitude should be distinguished from tidal range, which describes the difference between high and low water and is more directly related to spring-neap variability. When the events are separated into spring and neap tides, TSI is generally stronger during spring tides and weaker during neap tides (mean values of –44 cm and –30 cm, respectively), but with a substantial overlap between the groups. This overlap reflects that high tide magnitude and tidal range are not uniquely related in the data, so that higher neap tides may exceed lower spring tides in individual cases. Similarly, *Tien et al.* (2025) also reported higher surge (equivalent to NTR in the present study) during neap tides and lower surge during spring tides in idealized typhoon experiments.

3.2 Impact of SLR on tide-surge interaction (ISTSI)

We next investigate how TSI changes under SLR. Previous studies have assessed the temporal changes of TSI by comparing different decades using tide gauge observations. While no clear long-term change in TSI distribution was found (Haigh et al., 2010; Feng et al., 2019), minor changes have been noted (Feng et al., 2019), such as a shift in peak timing towards high tide at one gauge and slightly higher NTR at another. These subtle changes may indicate a minor weakening effect of SLR on TSI, though they are not consistent across locations and could be affected by decadal MSL and surge variabilities.

SLR effects on TSI could be quantified with our simulations. Computing NTR from the experiments under SLR (Table 2, Eq. (2)), Fig. 7 shows nearly unchanged distribution patterns compared to Fig. 2b, although the first peak becomes flatter and the second shifts one hour towards high tide. Although the chi-square test still confirms statistically significant deviation from the uniform distribution, the chi-square value decreases slightly, indicating that TSI persists but it weakens under 1 m SLR.

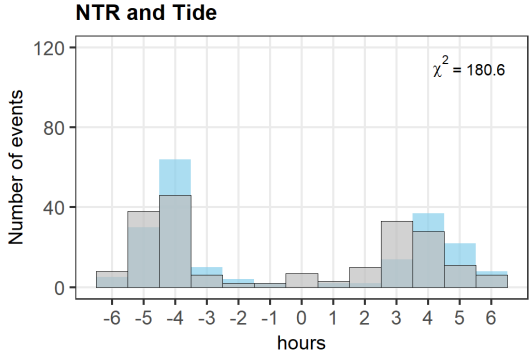

Figure 7. Frequency distribution of NTR peaks relative to the timing of high tide under 1 m SLR (gray bar). The light blue bar in the background is the distribution under no-SLR condition from Fig. 2b.

https://doi.org/10.5194/egusphere-2026-3871
Preprint. Discussion started: 8 July 2026

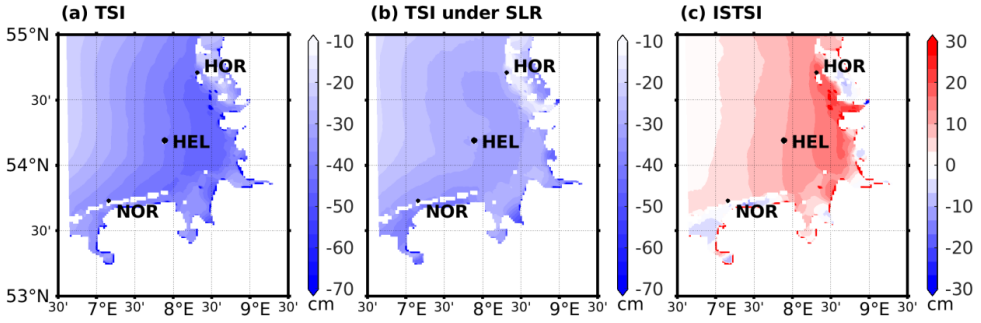

Figure 8. Maps of (a) TSI with no SLR, (b) TSI under 1 m SLR and (c) the SLR impact on TSI (ISTSI) at the nearest high tides of the surge events detected at three locations within a 1 h time window.

As can be inferred from Fig. 4 (orange curve), ISTSI is generally inversely related to the original TSI. When TSI reaches its minimum near high tide, SLR induces a positive TSI change, indicating a weakened nonlinear effect. This is a basin-wide effect, as is evident from Fig. 8. There the TSI under present-day and +1 m SLR conditions is estimated based on surge events co-occurring throughout the German Bight and detected at three locations within a 1 h time window (87 events). The event-averaged TSI becomes less negative under SLR compared to the control case, demonstrating a systematic weakening of TSI. This behaviour can be largely explained by the reduction of bottom friction associated with increased water depth. Reduced friction leads to lower energy dissipation, which tends to increase local water levels, while simultaneously weakening the nonlinear momentum exchange between tidal currents and surge flows. As a result, the coupling between tides and surges is reduced, and the system response becomes more linear (Idier et al., 2019).

The magnitude of this weakening is, however, small. Around high tide, TSI ranges from –65 cm to –9 cm (5^{th}–95^{th} percentiles) with only five positive cases and a mean value of about –38 cm (Fig. 9), consistent with values reported previously (Rego and Li, 2010; Song et al., 2020; Huang et al., 2025). More positive cases exist for TSI at surge peaks (Fig. 3a), because the effect is weaker at surge peaks. The ISTSI around high tide mostly lies between 2 cm and 15 cm, with only three negative cases and a mean of 10 cm. Thus, it reduces the original TSI by approximately 25 % on average.

https://doi.org/10.5194/egusphere-2026-3871
Preprint. Discussion started: 8 July 2026

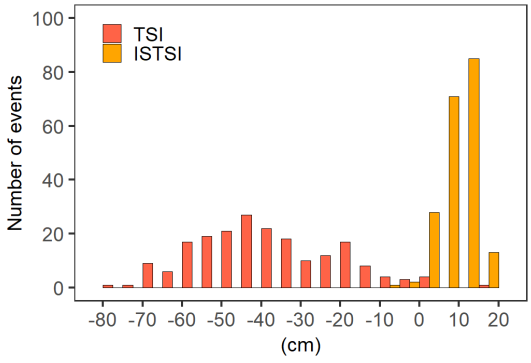

Figure 9. Frequency distribution of TSI with no SLR (red) and ISTSI (orange) at high tide.

3.3 Impact of SLR on storm surges (ISS)

The impact of SLR on storm surges is estimated from the two surge-only runs. The same wind forcing was used for both simulations, so their differences stem only from the change in MSL. In other words, the surge response reflects only SLR, independent of tides or atmospheric variations. Surge changes are determined as differences between corresponding peaks of the control run (SURGE_0) and the run with 1 m SLR (SURGE_1) as shown by Eq. (3). Surge changes due to SLR show an asymmetric distribution dominated by negative values (70 %), indicating on average a slight reduction in surge height in response to SLR (Fig. 10a). Figure 10b shows the spatial distribution of ISS for the coincident surge events detected at three locations within a 1 h time window, highlighting a basin-scale reduction in relative surge height under higher MSL. The reduction reflects a combination of two opposing depth-related effects as SLR increases total water depth: while this leads to reduced bottom friction and thus less dissipation, which tend to promote higher surge development, it also makes surface wind stress less effective by acting on a thicker water column, thereby dampening surge generation (e.g. Arns et al., 2017). The strongest negative response appears about 5 hours after the surge peak (Fig. 11), indicating a depth-induced phase shift caused by faster wave propagation in deeper water. As a result, surge height evaluated at the surge peak timestep is also slightly lower, although the difference is small and not easily visible in the surge curves in Fig. 11.

https://doi.org/10.5194/egusphere-2026-3871
Preprint. Discussion started: 8 July 2026

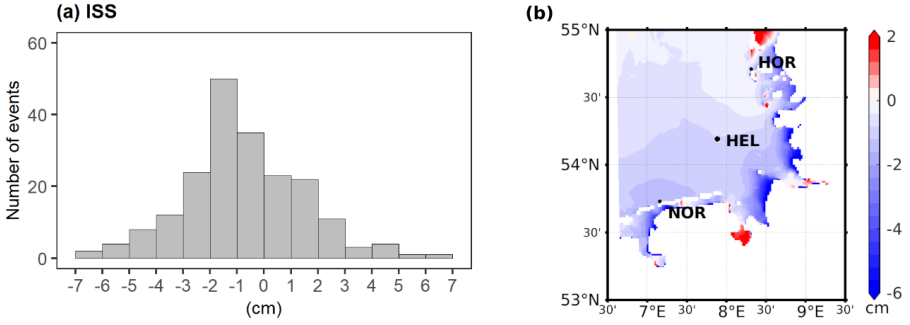

Figure 10. (a) Frequency distribution of the impact of SLR on storm surges (ISS). (b) Map of ISS for the surge events detected at three locations within a 1 h time window.

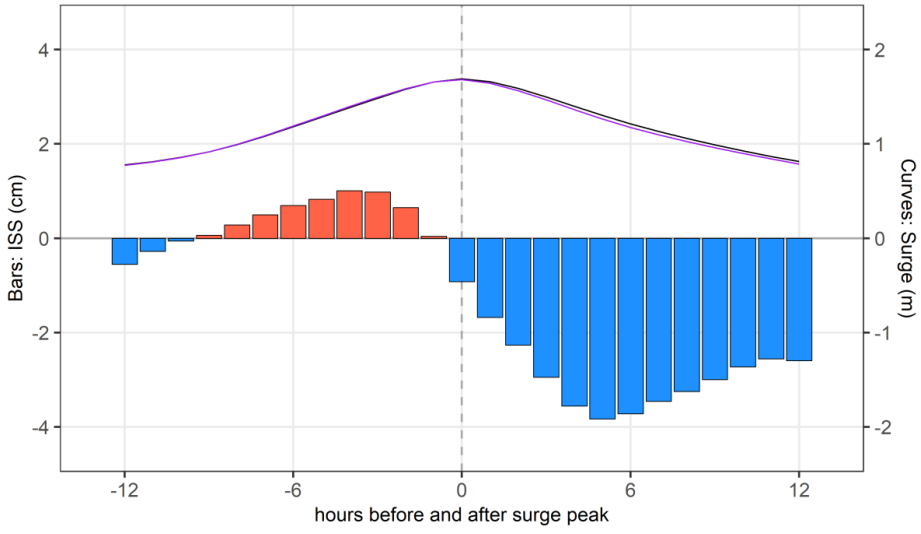

Figure 11. Event-averaged ISS (bars, cm), shown relative to the timing of surge peaks (gray dashed line). The curves (m) represent storm surge (black) and storm surge under SLR minus 1 m (purple).

The reduction is on the order of centimeters for 1 m SLR, comparable to the SLR impact on TSI at surge peaks (Fig. 4). On average, surge maxima decrease by about 1 %. Most of the strongest reductions fall between −3 cm and −8 cm (5^{th}–95^{th} percentiles), with a mean of −5 cm (Fig. 12). Larger reductions occur during stronger surge events, suggesting that stronger currents enhance the underlying interactions. Overall, these results demonstrate that TSI is a dominant control on both the timing and magnitude of surge-related water

https://doi.org/10.5194/egusphere-2026-3871
Preprint. Discussion started: 8 July 2026

levels. In contrast, the effects of SLR on these processes are comparatively small, although systematic and physically consistent.

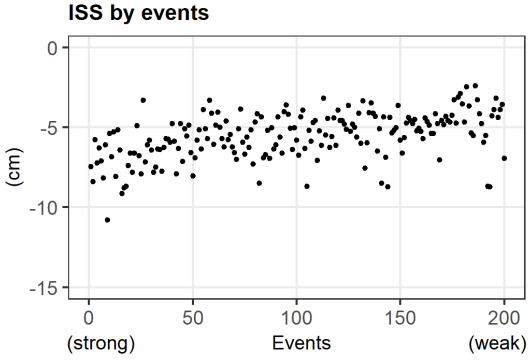

Figure 12. The maximum reduction of ISS, ordered from highest to lowest surge.

3.4 Impact of SLR on tides (IST)

Changes in tidal dynamics due to SLR were not the main scope of this study. However, to ensure consistency and to set our results into the context of previous studies, an analysis of changes in high tide under SLR was made based on the tide-only simulations with and without SLR described in Section 2.3. For that we compared high tide magnitudes associated with the highest 200 storm surge events analyzed in Section 3. Figure 13 shows a mean difference of these high tides deviating from the SLR magnitude. High tide decreases in response to SLR for the offshore areas of the German Bight, especially in the eastern part and increases for the shallow areas of the Wadden Sea. This pattern generally agrees with the pattern of the M2 amplitude changes due to a SLR of 0.8 m shown by *Rasquin et al.* (2020) or SLR of 0.8 m and 2 m shown by *Jordan et al.* (2021).

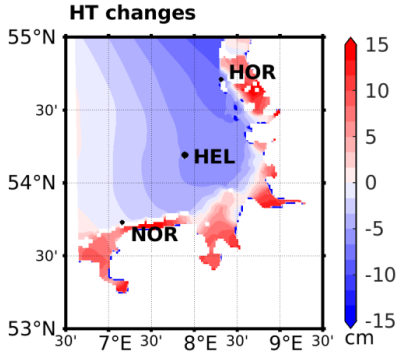

https://doi.org/10.5194/egusphere-2026-3871
Preprint. Discussion started: 8 July 2026

Figure 13. Map of high tide changes in response to SLR.

4 Discussion

4.1 High tide changes due to SLR

As can be inferred from previous studies, the response of the M2 tidal amplitude and high water level to SLR is strongly dependent on experimental design. In particular, the representation of coastal geometry plays a key role: simulations that allow coastal flooding produce markedly different spatial patterns compared to those assuming rigid coastlines (e.g. Pelling et al., 2013; Idier et al., 2017), with the present study being closer to the latter configuration. Additionally, the resolution of the underlying bathymetry, and likely the numerical model resolution itself, influence the response on a qualitative level (Rasquin et al., 2020). They have demonstrated that the larger increase in dissipation rate in the fine bathymetry model is largely due to overall increased current speeds, which cannot be seen to the same extent from a coarse bathymetry model. Overall, the response of tides on SLR in the German Bight is collectively determined by the interplay of the reduced dampening of high water due to increased water depth and the consequent weakening of bottom friction, increased dissipation rates due to finer resolution and additional increase in dissipation due to depth reduction when coastal flooding of grid cells is considered.

Moreover, the magnitude of the imposed SLR further modulates the spatial pattern of M2 amplitude and high tide changes. Under moderate SLR (approximately 0.8–1 m), a substantial part of the German Bight exhibits a reduction in M2 amplitude when estimated with finer bathymetry resolution (Rasquin et al., 2020; Jordan et al., 2021), and an increase in M2 amplitude (or high water) when coarser bathymetry is implied (Idier et al., 2017; Rasquin et al., 2020). For higher SLR scenarios (typically 2 m), the area of reduced amplitude diminishes and shifts northward (Pelling et al., 2013; Idier et al., 2017; Jordan et al., 2021). In contrast, extreme SLR scenarios (5–10 m) lead to a consistent positive-valued signal in M2 amplitude (Rasquin et al., 2020) or maximum high water (Idier et al., 2017) across the German Bight independently on the bathymetry resolution. For the moderate SLR scenario considered in the present study, the spatial pattern of changes is consistent with the general consensus of the abovementioned studies concerning the response of M2 amplitude. It should be noted, however, that present study focuses on high tides across the full tidal spectrum rather than directly on M2 amplitude. These metrics are not equivalent, as high tides reflect the combined effect of multiple tidal constituents but obviously omit the low tide changes, which directly affect tidal amplitude.

https://doi.org/10.5194/egusphere-2026-3871
Preprint. Discussion started: 8 July 2026

4.2 Importance of timing

We show statistically that the most pronounced negative TSI values occur mostly near high tide, not at the surge peaks, and the oscillation of TSI is highly dependent on the tidal phases. The average TSI is about –38 cm near high tide, and –21 cm at the surge peaks. Similar values of TSI were reported in previous studies. *Rego and Li* (2010) showed TSI are –30 cm at high tides for the diurnal tide simulations and –40 cm for the semidiurnal cases in their case study. The values are also comparable to the value of –32 cm reported previously in a case study (Song et al., 2020) and fall within the ranges of another case study of *Huang et al.* (2025). *Zhang et al.* (2017) focused on the TSI at surge peaks and highlighted the modification of tidal phases on the maximum surges. In their analysis of multiple typhoon events, TSI was found to dampen the surge peak near high tide and to enhance it when occurred during low tide by about 15–25 %. They also underscored that the TSI increases the duration of storm surge while reducing the maximum surge, and vice versa for the low tide cases. Although water level enhancement during low tide may not be critical for EWLs, it can prolong the periods of elevated low water during long-lasting storm surge events that span several tidal cycles. This may pose challenges for the drainage of low-lying coastal areas, as well as increase the risk of compound flooding by limiting discharge capacity (e.g. Bormann et al., 2024).

4.3 EWL changes, attribution and limitations

Taken together, the results highlight that SLR influences EWLs through changes in tides (IST), storm surges (ISS), and their nonlinear interaction (ISTSI), which need to be interpreted jointly to understand the total response. In particular, a weakening of TSI under SLR (Fig. 8 and 9) reduces its dampening effect on water level, contributing to higher extremes. As shown in Fig. 14, WL changes due to +1 m SLR are largely concentrated between –1 cm to 7 cm (5^{th}–95^{th} percentiles). The changes are in similar order of magnitude as shown, e.g., by *Idier et al.* (2017). These changes exhibit a linear dependence on ISTSI, indicating that the increase in water level beyond SLR alone can be attributed to the weakening of the negative TSI effect under SLR. Detected response may, however, differ significantly when larger SLR is considered (5–10 m), as is indicated, e.g., by *Idier et al.* (2017) or *Rasquin et al.* (2020). We explicitly omit these low probability scenarios (Fox-Kemper et al., 2021) in order to concentrate on results and processes more relevant for the coming decades rather than centuries.

It is also worth mentioning that changes in EWL are the result of many factors. Here we only discussed the nonlinear changes and effects of TSI related to the increased MSL, while it is not the only parameter changing with time or climate state. One process indirectly linked to the changing MSL and not considered in the present study is the potential change in bathymetry due to natural variability as well as altering of sediment transport patterns under SLR (Huismans et al., 2022). This may be of particular importance for the EWL changes in shallow areas, and so

https://doi.org/10.5194/egusphere-2026-3871
Preprint. Discussion started: 8 July 2026

far the effect is inconclusive, especially considering the large uncertainty regarding the reaction of intertidal flats to SLR. Another major contributor to the changing EWL is the change in wind climate and storminess, which may directly trigger changes in storm surge magnitude under the climate change conditions (Lowe et al., 2001; Gaslikova et al., 2013; Vousdoukas et al., 2016) but are out of the scope of present study.

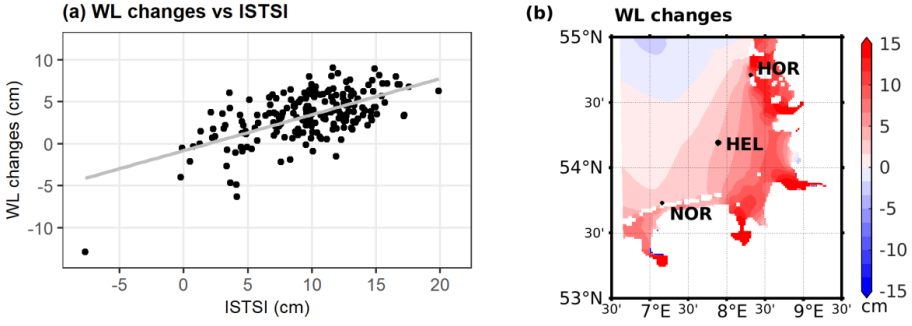

Figure 14. (a) Scatter plot of WL changes due to SLR versus ISTSI with fitted regression line. (b) Map of WL changes due to SLR.

4.4 Nonlinear versus linear

Finally, this study also aims to quantify uncertainty in estimating absolute EWLs under SLR conditions, which arises from the linear consideration of different WL components as opposed to a dynamical combination that accounts for nonlinear interactions. For that four configurations of EWL estimate are compared (Fig. 15) ranging from fully dynamic (WL_SLR) to fully linear (Linera_0). The statistics of the present-day WL linearly combined with 1 m SLR (WL+SLR) and the dynamically simulated WL under SLR (WL_SLR) are close to each other, with the mean values underestimated by about 1 % in case of linear combination. Larger differences emerge under surge conditions (Fig. 15a) when tide, surge and 1 m SLR are all added linearly (Linear_0), thus omitting surge-tide-SLR interactions altogether, and when surge-SLR and tide-SLR interactions are considered by using the sum of tide and surge under SLR (Linear_1). Both approaches exclude TSI processes and overestimate the mean WL_SLR by about 11 % and 9 %, respectively. Under non-surge conditions (Fig. 15b), the statistics of the four estimates are very similar to each other, with the largest difference of about 4 % occurring also between the fully dynamic and fully linear estimates.

These results highlight the importance of TSI as a source of uncertainty in water level simulations. The nonlinear effects of SLR on oceanic components remain small (1–2 %), even under surge conditions, corresponding to a few centimeters for 1 m SLR. However, these effects are systematic and therefore relevant for process understanding and uncertainty

https://doi.org/10.5194/egusphere-2026-3871
Preprint. Discussion started: 8 July 2026

quantification. This is consistent with earlier studies showing limited nonlinear influence of SLR on surge propagation (Lowe et al., 2001; Sterl et al., 2009).

Overall, nonlinear processes do not invalidate linear superposition approaches but instead define the associated uncertainty. Consequently, the inclusion of nonlinear effects depends on the application: linear addition of SLR is sufficient for many practical purposes, whereas nonlinear processes primarily introduce small but systematic deviations that are relevant for more precise assessments.

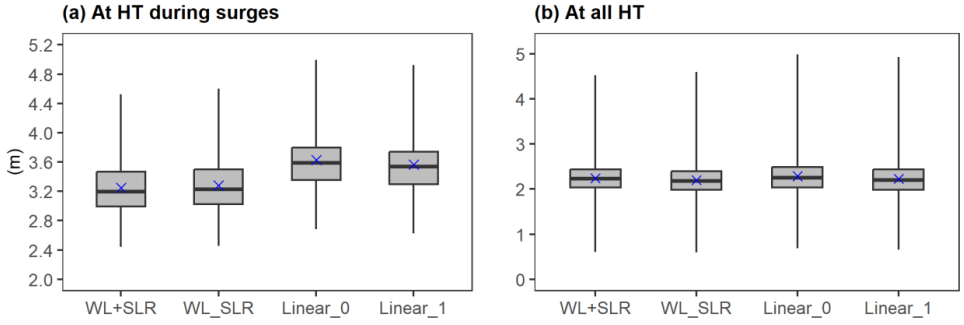

Figure 15. Boxplots of water levels (a) at high tides under surge condition and (b) at all high tides: FULL_0 plus 1 m SLR linearly (WL+SLR), FULL_1 from the dynamical run with SLR (WL_SLR), linear sum of TIDE_0, SURGE_0 and 1 m SLR (Linear_0), and linear sum of TIDE_1 and SURGE_1 minus 1 m (Linear_1). The boxplot displays the minimum, 25th percentile, median, 75th percentile and maximum values, and the blue cross marks the mean.

5 Conclusions

This study investigates how sea level rise (SLR) modifies storm surges and tide-surge interaction (TSI) in the German Bight, with the aim of assessing the relevance of nonlinear processes for estimating extreme water levels (EWLs). Using long-term hydrodynamic simulations and sensitivity experiments, we separated tidal, meteorological, and interaction effects and quantified their response to a +1 m SLR scenario.

Our analysis shows that the influence of TSI on storm surge height and timing is strongly controlled by tidal phases. The largest dampening occurs when surge peaks coincide with high tide, while the interaction is weaker and occasionally constructive near low tide. In addition, TSI shifts peak surge levels away from high tide, further modifying the temporal structure of extreme events. The strength of TSI increases with surge magnitude, whereas its dependence on tidal characteristics such as high tide level or tidal range is comparatively weak and more variable.

https://doi.org/10.5194/egusphere-2026-3871
Preprint. Discussion started: 8 July 2026

Under SLR, the negative effect of TSI is slightly weaker. This reduction in nonlinear interaction is consistent with the water depth increase and the associated decrease in bottom friction, which leads to a more linear system response. The weakening primarily manifests as a reduction of the negative TSI signal by about 10 cm on average, corresponding to a decrease of roughly one quarter of its present-day magnitude. As a consequence, the dampening effect of TSI on surge-related water levels is reduced under SLR. This contributes to an increase in total water level beyond SLR alone, although the effect remains small compared to the direct SLR contribution.

Moreover, storm surge heights decrease slightly under SLR when considered as a stand-alone process. This reduction is small (a few centimeters for 1 m SLR) and is attributed to two depth-related mechanisms: a phase shift associated with faster wave propagation in deeper water and the reduced efficiency of wind stress in driving a thicker water column. The magnitude of this effect scales with surge intensity but remains small in absolute terms.

In summary, this study demonstrates that TSI contributes largely to the uncertainties in water level simulations, whereas nonlinear SLR effects are small but play a systematic role in shaping the dynamics and associated uncertainties in shallow coastal seas. The findings support the use of linear superposition of SLR and present-day EWL estimates for many applications. Meanwhile, they highlight that nonlinear interactions introduce process-based adjustments, which are particularly relevant for a detailed understanding of coastal dynamics and for quantifying uncertainties in high-precision applications, such as coastal protection design or attribution studies.

Data availability. The model outputs used in this study are available upon request from the authors.

Author contributions. XL performed the analysis. All authors contributed to the study design, analysis discussion and manuscript preparation.

Competing interests. The authors declare that they have no conflict of interest.

Acknowledgements.

Financial support. This work was funded by the Federal Ministry for Research, Technology and Space (BMFTR) through the research project ClimXtreme II. The article processing charges for this open-access publication were covered by the Helmholtz-Zentrum Hereon.

https://doi.org/10.5194/egusphere-2026-3871
Preprint. Discussion started: 8 July 2026

References

Arns, A., Wahl, T., Dangendorf, S., and Jensen, J.: The impact of sea level rise on storm surge water levels in the northern part of the German Bight, Coastal Engineering, 96, 118–131, https://doi.org/10.1016/j.coastaleng.2014.12.002, 2015.

Arns, A., Dangendorf, S., Jensen, J., Talke, S., Bender, J., and Pattiaratchi, C.: Sea-level rise induced amplification of coastal protection design heights, Sci. Rep., 7, https://doi.org/10.1038/srep40171, 2017.

Arns, A., Wahl, T., Wolff, C., Vafeidis, A. T., Haigh, I. D., Woodworth, P., Niehüser, S., and Jensen, J.: Non-linear interaction modulates global extreme sea levels, coastal flood exposure, and impacts, Nat. Commun., 11, 1918, https://doi.org/10.1038/s41467-020-15752-5, 2020.

Bormann, H., Kebschull, J., Gaslikova, L., and Weisse, R.: Model-based assessment of climate change impact on inland flood risk at the German North Sea coast caused by compounding storm tide and precipitation events, Nat. Hazards Earth Syst. Sci., 24, 2559–2576, https://doi.org/10.5194/nhess-24-2559-2024, 2024.

Bruss, G., Gönnert, G., and Mayerle, R.: Extreme scenarios at the German north sea coast a numerical model study, Int. Conf. Coastal. Eng., 1(32), currents.26, https://doi.org/10.9753/icce.v32.currents.26, 2011.

Casulli Vincenzo and Stelling Guus S.: Numerical Simulation of 3D Quasi-Hydrostatic, Free-Surface Flows, Journal of Hydraulic Engineering, 124, 678–686, https://doi.org/10.1061/(ASCE)0733-9429(1998)124:7(678), 1998.

Codiga, D.L.: Unified Tidal Analysis and Prediction Using the UTide Matlab Functions, Technical Report 2011-01, Graduate School of Oceanography, University of Rhode Island, Narragansett, RI. 59pp. ftp://www.po.gso.uri.edu/pub/downloads/codiga/pubs/2011Codiga-UTide-Report.pdf, 2011.

Feng, J., Jiang, W., Li, D., Liu, Q., Wang, H., and Liu, K.: Characteristics of tide–surge interaction and its roles in the distribution of surge residuals along the coast of China, J. Oceanogr., 75, 225–234, https://doi.org/10.1007/s10872-018-0495-8, 2019.

Feng, X., Olabarrieta, M., and Valle-Levinson, A.: Storm-induced semidiurnal perturbations to surges on the US Eastern Seaboard, Cont. Shelf Res., 114, 54–71, https://doi.org/10.1016/j.csr.2015.12.006, 2016.

Fox-Kemper, B., H.T. Hewitt, C. Xiao, G. Aðalgeirsdóttir, S.S. Drijfhout, T.L. Edwards, N.R. Golledge, M. Hemer, R.E. Kopp, G. Krinner, A. Mix, D. Notz, S. Nowicki, I.S. Nurhati, L. Ruiz, J.-B. Sallée, A.B.A. Slangen, and Y. Yu: Ocean, Cryosphere and Sea Level Change. In Climate Change 2021: The Physical Science Basis. Contribution of Working Group I to the Sixth Assessment Report of the Intergovernmental Panel on Climate Change [Masson-Delmotte, V., P. Zhai, A.

https://doi.org/10.5194/egusphere-2026-3871
Preprint. Discussion started: 8 July 2026

Pirani, S.L. Connors, C. Péan, S. Berger, N. Caud, Y. Chen, L. Goldfarb, M.I. Gomis, M. Huang, K. Leitzell, E. Lonnoy, J.B.R. Matthews, T.K. Maycock, T. Waterfield, O. Yelekçi, R. Yu, and B. Zhou (eds.)]. Cambridge University Press, Cambridge, United Kingdom and New York, NY, USA, pp. 1211–1362, https://doi.org/10.1017/9781009157896.011, 2011.

Garner, G. G., T. Hermans, R. E. Kopp, A. B. A. Slangen, T. L. Edwards, A. Levermann, S. Nowikci, M. D. Palmer, C. Smith, B. Fox-Kemper, H. T. Hewitt, C. Xiao, G. Aðalgeirsdóttir, S. S. Drijfhout, T. L. Edwards, N. R. Golledge, M. Hemer, G. Krinner, A. Mix, D. Notz, S. Nowicki, I. S. Nurhati, L. Ruiz, J-B. Sallée, Y. Yu, L. Hua, T. Palmer, B. Pearson: IPCC AR6 Sea Level Projections, Version 20210809, Dataset accessed [2026-02-10] at https://doi.org/10.5281/zenodo.5914709, 2021.

Gaslikova, L., Grabemann, I., and Groll, N.: Changes in North Sea storm surge conditions for four transient future climate realizations, Nat. Hazards, 66, 1501–1518, https://doi.org/10.1007/s11069-012-0279-1, 2013.

Geyer, B.: High-resolution atmospheric reconstruction for Europe 1948–2012: coastDat2, Earth Syst. Sci. Data, 6, 147–164, https://doi.org/10.5194/essd-6-147-2014, 2014.

Haigh, I., Nicholls, R., and Wells, N.: Assessing changes in extreme sea levels: Application to the English Channel, 1900–2006, Cont. Shelf Res., 30, 1042–1055, https://doi.org/10.1016/j.csr.2010.02.002, 2010.

Horsburgh, K. J. and Wilson, C.: Tide-surge interaction and its role in the distribution of surge residuals in the North Sea, J. Geophys. Res.-Oceans, 112, https://doi.org/10.1029/2006jc004033, 2007.

Huang, L., Zhang, T., Zhang, S., and Wang, H.: Effect of nonlinear tide–surge interaction in the Pearl River Estuary during Typhoon Nida (2016), Ocean Sci., 21, 1891–1908, https://doi.org/10.5194/os-21-1891-2025, 2025.

Huismans, Y., van der Spek, A., Lodder, Q., Zijlstra, R., Elias, E., and Wang, Z. B.: Development of intertidal flats in the Dutch Wadden Sea in response to a rising sea level: Spatial differentiation and sensitivity to the rate of sea level rise, Ocean & Coastal Management, 216, 105969, https://doi.org/10.1016/j.ocecoaman.2021.105969, 2022.

Hunter, J.: Estimating sea-level extremes under conditions of uncertain sea-level rise, Climatic Change, 99, 331–350, https://doi.org/10.1007/s10584-009-9671-6, 2010.

Idier, D., Dumas, F., and Muller, H.: Tide-surge interaction in the English Channel, Nat. Hazards Earth Syst. Sci., 12, 3709–3718, https://doi.org/10.5194/nhess-12-3709-2012, 2012.

Idier, D., Paris, F., Cozannet, G. L., Boulahya, F., and Dumas, F.: Sea-level rise impacts on the tides of the European Shelf, Cont. Shelf Res., 137, 56–71, https://doi.org/10.1016/j.csr.2017.01.007, 2017.

https://doi.org/10.5194/egusphere-2026-3871
Preprint. Discussion started: 8 July 2026

Idier, D., Bertin, X., Thompson, P., and Pickering, M. D.: Interactions Between Mean Sea Level, Tide, Surge, Waves and Flooding: Mechanisms and Contributions to Sea Level Variations at the Coast, Surv. Geophys., 40, 1603–1630, https://doi.org/10.1007/s10712-019-09549-5, 2019.

Jordan, C., Visscher, J., and Schlurmann, T.: Projected Responses of Tidal Dynamics in the North Sea to Sea-Level Rise and Morphological Changes in the Wadden Sea, Frontiers in Marine Sci., 8, https://doi.org/10.3389/fmars.2021.685758, 2021.

Kapitza, H.: MOPS – a morphodynamical prediction system on cluster computers. In: High performance computing for computational science – VECPAR 2008, edited by: Laginha, J. M., Palma, M., Amestoy, P. R., Dayde, M., Mattoso, M., and Lopez, J., 63–68, https://doi.org/10.1007/978-3-540-92859-1_8, 2008.

Katsman, C. A., Sterl, A., Beersma, J. J., van den Brink, H. W., Church, J. A., Hazeleger, W., Kopp, R. E., Kroon, D., Kwadijk, J., Lammersen, R., Lowe, J., Oppenheimer, M., Plag, H.-P., Ridley, J., von Storch, H., Vaughan, D. G., Vellinga, P., Vermeersen, L. L. A., van de Wal, R. S. W., and Weisse, R.: Exploring high-end scenarios for local sea level rise to develop flood protection strategies for a low-lying delta—the Netherlands as an example, Climatic Change, 109, 617–645, https://doi.org/10.1007/s10584-011-0037-5, 2011.

Kopp, R. E., Garner, G. G., Hermans, T. H. J., Jha, S., Kumar, P., Reedy, A., Slangen, A. B. A., Turilli, M., Edwards, T. L., Gregory, J. M., Koubbe, G., Levermann, A., Merzky, A., Nowicki, S., Palmer, M. D., and Smith, C.: The Framework for Assessing Changes To Sea-level (FACTS) v1.0: a platform for characterizing parametric and structural uncertainty in future global, relative, and extreme sea-level change, Geoscientific Model Development, 16, 7461–7489, https://doi.org/10.5194/gmd-16-7461-2023, 2023.

Lowe, J. A., Gregory, J. M., and Flather, R. A.: Changes in the occurrence of storm surges around the United Kingdom under a future climate scenario using a dynamic storm surge model driven by the Hadley Centre climate models, Clim. Dynam., 18, 179–188, https://doi.org/10.1007/s003820100163, 2001.

Lyard, F., Lefevre, F., Letellier, T., and Francis, O.: Modelling the global ocean tides: modern insights from FES2004, Ocean Dynam., 56, 394–415, https://doi.org/10.1007/s10236-006-0086-x, 2006.

Meyer, E. M. I. and Gaslikova, L.: Investigation of historical severe storms and storm tides in the German Bight with century reanalysis data, Nat. Hazards Earth Syst. Sci., 24, 481–499, https://doi.org/10.5194/nhess-24-481-2024, 2024.

Olbert, A. I., Nash, S., Cunnane, C., and Hartnett, M.: Tide–surge interactions and their effects on total sea levels in Irish coastal waters, Ocean Dynam., 63, 599–614, https://doi.org/10.1007/s10236-013-0618-0, 2013.

https://doi.org/10.5194/egusphere-2026-3871
Preprint. Discussion started: 8 July 2026

Pätsch, J., Burchard, H., Dieterich, C., Gräwe, U., Gröger, M., Mathis, M., Kapitza, H., Bersch, M., Moll, A., Pohlmann, T., Su, J., Ho-Hagemann, H. T. M., Schulz, A., Elizalde, A., and Eden, C.: An evaluation of the North Sea circulation in global and regional models relevant for ecosystem simulations, Ocean Modelling, 116, 70–95, https://doi.org/10.1016/j.ocemod.2017.06.005, 2017.

Pelling, H. E., Mattias Green, J. A., and Ward, S. L.: Modelling tides and sea-level rise: To flood or not to flood, Ocean Modelling, 63, 21–29, https://doi.org/10.1016/j.ocemod.2012.12.004, 2013.

Pickering, M. D., Wells, N. C., Horsburgh, K. J., and Green, J. A. M.: The impact of future sea-level rise on the European Shelf tides, Cont. Shelf Res., 35, 1–15, https://doi.org/10.1016/j.csr.2011.11.011, 2012.

Prandle, D. and Wolf, J.: The interaction of surge and tide in the North Sea and River Thames, Geophysical Journal International, 55, 203–216, https://doi.org/10.1111/j.1365-246X.1978.tb04758.x, 1978.

Quinn, N., Atkinson, P. M., and Wells, N. C.: Modelling of tide and surge elevations in the Solent and surrounding waters: The importance of tide–surge interactions, Estuar. Coast. Shelf Sci., 112, 162–172, https://doi.org/10.1016/j.ecss.2012.07.011, 2012.

Rasquin, C., Seiffert, R., Wachler, B., and Winkel, N.: The significance of coastal bathymetry representation for modelling the tidal response to mean sea level rise in the German Bight, Ocean Sci., 16, 31–44, https://doi.org/10.5194/os-16-31-2020, 2020.

Rego, J. L. and Li, C.: Nonlinear terms in storm surge predictions: Effect of tide and shelf geometry with case study from Hurricane Rita, J. Geophys. Res.-Oceans, 115, https://doi.org/10.1029/2009JC005285, 2010.

Santamaria-Aguilar, S., Arns, A., and Vafeidis, A. T.: Sea-level rise impacts on the temporal and spatial variability of extreme water levels: A case study for St. Peter-Ording, Germany, J. Geophys. Res.-Oceans, 122, 2742–2759, https://doi.org/10.1002/2016JC012579, 2017.

Smith, S. D. and Banke, E. G.: Variation of the sea surface drag coefficient with wind speed, Quarterly Journal of the Royal Meteorological Society, 101, 665–673, https://doi.org/10.1002/qj.49710142920, 1975.

Song, H., Kuang, C., Gu, J., Zou, Q., Liang, H., Sun, X., and Ma, Z.: Nonlinear tide-surge-wave interaction at a shallow coast with large scale sequential harbor constructions, Estuar. Coast. Shelf Sci., 233, 106543, https://doi.org/10.1016/j.ecss.2019.106543, 2020.

Sterl, A., van den Brink, H., de Vries, H., Haarsma, R., and van Meijgaard, E.: An ensemble study of extreme storm surge related water levels in the North Sea in a changing climate, Ocean Sci., 5, 369–378, https://doi.org/10.5194/os-5-369-2009, 2009.

https://doi.org/10.5194/egusphere-2026-3871
Preprint. Discussion started: 8 July 2026

Taherkhani, M., Vitousek, S., Barnard, P. L., Frazer, N., Anderson, T. R., and Fletcher, C. H.: Sea-level rise exponentially increases coastal flood frequency, Sci. Rep., 10, 6466, https://doi.org/10.1038/s41598-020-62188-4, 2020.

Tien, P. V., Thuy, N. B., Kim, S., Cuong, N. K., Ngoc, P. K., Khiem, M. V., and Hole, L. R.: Impact of the interaction of surge, wave, and tide on the surge and wave on the northern coast of Vietnam for a marine storm surge and wave forecast system, Regional Studies in Marine Science, 87, 104234, https://doi.org/10.1016/j.rsma.2025.104234, 2025.

Vousdoukas, M. I., Voukouvalas, E., Annunziato, A., Giardino, A., and Feyen, L.: Projections of extreme storm surge levels along Europe, Clim. Dynam., 47, 3171–3190, https://doi.org/10.1007/s00382-016-3019-5, 2016.

Vousdoukas, M. I., Mentaschi, L., Voukouvalas, E., Verlaan, M., and Feyen, L.: Extreme sea levels on the rise along Europe's coasts, Earth's Future, 5, 304–323, https://doi.org/10.1002/2016EF000505, 2017.

Ward, S. L., Green, J. A. M., and Pelling, H. E.: Tides, sea-level rise and tidal power extraction on the European shelf, Ocean Dynam., 62, 1153–1167, https://doi.org/10.1007/s10236-012-0552-6, 2012.

Weisse, R., von Storch, H., Niemeyer, H. D., and Knaack, H.: Changing North Sea storm surge climate: An increasing hazard?, Ocean & Coastal Management, 68, 58–68, https://doi.org/10.1016/j.ocecoaman.2011.09.005, 2012.

Weisse, R., Bellafiore, D., Menéndez, M., Méndez, F., Nicholls, R. J., Umgiesser, G., and Willems, P.: Changing extreme sea levels along European coasts, Coastal Engineering, 87, 4–14, https://doi.org/10.1016/j.coastaleng.2013.10.017, 2014.

Weisse, R., Bisling, P., Gaslikova, L., Geyer, B., Groll, N., Hortamani, M., Matthias, V., Maneke, M., Meinke, I., Meyer, E. M., Schwichtenberg, F., Stempinski, F., Wiese, F., and Wöckner-Kluwe, K.: Climate services for marine applications in Europe, Earth Perspectives, 2, 3, https://doi.org/10.1186/s40322-015-0029-0, 2015.

Zhang, H., Cheng, W., Qiu, X., Feng, X., and Gong, W.: Tide-surge interaction along the east coast of the Leizhou Peninsula, South China Sea, Cont. Shelf Res., 142, 32–49, https://doi.org/10.1016/j.csr.2017.05.015, 2017.

Zijl, F., Verlaan, M., and Gerritsen, H.: Improved water-level forecasting for the Northwest European Shelf and North Sea through direct modelling of tide, surge and non-linear interaction, Ocean Dynam., 63, 823–847, https://doi.org/10.1007/s10236-013-0624-2, 2013.